Review Paper

Recent advances in cancer photo-theranostics: the synergistic combination of transition metal complexes and gold nanostructures

Loredana Ricciardi[1] · Massimo La Deda[2]

Received: 14 December 2020 / Accepted: 2 February 2021

Abstract
In this mini review, we highlight advances in the last five years in light-activated cancer theranostics by using hybrid systems consisting of transition metal complexes (TMCs) and plasmonic gold nanostructures (AuNPs). TMCs are molecules with attractive properties and high potential in biomedical application. Due to their antiproliferative abilities, platinum-based compounds are currently first-choice drugs for the treatment of several solid tumors. Moreover, ruthenium, iridium and platinum complexes are well-known for their ability to photogenerate singlet oxygen, a highly cytotoxic reactive species with a key role in photodynamic therapy. Their potential is further extended by the unique photophysical properties, which make TMCs particularly suitable for bioimaging. Recently, gold nanoparticles (AuNPs) have been widely investigated as one of the leading nanomaterials in cancer theranostics. AuNPs—being an inert and highly biocompatible material—represent excellent drug delivery systems, overcoming most of the side effects associated with the systemic administration of anticancer drugs. Furthermore, due to the thermoplasmonic properties, AuNPs proved to be efficient nano-sources of heat for photothermal therapy application. Therefore, the hybrid combination TMC/AuNPs could represent a synergistic merger of multiple functionalities for combinatorial cancer therapy strategies. Herein, we report the most recent examples of TMC/AuNPs systems in in-vitro in-vivo cancer tharanostics application whose effects are triggered by light-exposure in the Vis–NIR region, leading to a spatial and temporal control of the TMC/AuNPs activation for light-mediated precision therapeutics.

Keywords Transition metal complexes · Gold nanoparticles · Light-mediated activation · Cancer theranostics

1 Introduction

Over the years, transition metal complexes (TMCs) have attracted growing attention as promising theranostic agents for cancer disease [1, 2]. Since the discovery of the antiproliferative properties of cisplatin in the 1960s [3], platinum-based agents have been widely administered in cancer therapy to treat different types of solid tumors [4], currently covering almost 50% of all the clinically used chemotherapy drugs. The mechanism of action underlying the therapeutic efficacy of the platinum compounds approved by FDA is based on their ability to stably bind the nuclear DNA of cancer cells, preventing their replication [4–8]. Nevertheless, the potential of TMCs in cancer medicine has proved to be much more than as mere chemotherapeutics. The presence of heavy metal atoms introduces attractive chemical and photophysical properties, leading—with the choice of proper ligands and metal ions—to luminescent compounds with high emission quantum yields, tunable emission color in the visible region, long excited state lifetimes and large Stokes shifts, properties very useful in biosensing and bioimaging

✉ Loredana Ricciardi, loredana.ricciardi@cnr.it; ✉ Massimo La Deda, massimo.ladeda@unical.it | [1]CNR NANOTEC - Institute of Nanotechnology, UOS Cosenza, 87036 Arcavacata di Rende, CS, Italy. [2]Department of Chemistry and Chemical Technologies, University of Calabria, 87036 Rende, CS, Italy.

SN Applied Sciences (2021) 3:372 | https://doi.org/10.1007/s42452-021-04329-6

Published online: 24 February 2021

[9–13]. Because of that, ruthenium [14–20], iridium [21–29] and platinum [30–35] complexes have been successfully employed as in-vitro and in-vivo luminescent biolabels. Moreover, as a consequence of the strong spin–orbit coupling due to the presence of the heavy atom, the intersystem crossing processes lead to an efficient population of energetically low-lying triplet excited states, often very close to the excited states of molecular oxygen, with consequent energy transfer processes and generation of singlet oxygen. Accordingly, the last decade has seen a dramatic expansion in the investigation of TMCs as photosensitizers in one- and two-photon photodynamic therapy (PDT) [11, 36–45]—with the first Ru(II)-based photosensitizer entered into human clinical trials in early 2017 for treating non-muscle invasive bladder cancer [46]. Finally, TMCs can be synthesized by combining different ligands and metal centers offering a wide range of oxidation states, coordination numbers and geometries. This molecular versatility can be employed to design site-specific stimuli-responsive prodrugs [47] and novel multifunctional scaffolds suitable for "all-in-one" cancer theranostic approaches [1].

Last few years have seen an exceptional growth in research and application of nanomaterials in cancer theranostics [48–50]. In this field, gold nanoparticles (AuNPs) have emerged as multifaceted platforms for combinatorial cancer therapy strategies [51–53]. Inert and highly biocompatible, AuNPs are—like other nanoscale materials—able to passively accumulate in the tumor site via enhanced permeability and retention (EPR) effect [54–56]; moreover, their surface can be easily functionalized with active targeting moieties leading to efficient nanocarriers for target-specific delivery of therapeutic agents [57]. Finally, their physicochemical properties can provide spatio-temporal control over the payloads release through internal (i.e. pH) or external stimuli (i.e. light) [57]. An important physical feature of AuNPs involves the localized surface plasmon resonance (LSPR)[58]. When electromagnetic radiation impinges metal nanoparticles smaller than incident wavelength, the surface electrons undergo a collective coherent oscillation in resonance with the electromagnetic field, causing absorption and scattering of the radiation at the resonant frequency. The latter depends on the size and shape of the nanostructure and generally falls within the Vis–NIR range [58]. As a consequence, plasmonic properties of AuNPs can be properly tuned and engineered changing their morphology [59–64]. Noteworthy, the interaction between the plasmonic field—generated by AuNPs—and proximal fluorophores, can tune the molecular luminescence, leading to additional interesting effects [65–69]. Moreover, as a result of the optical energy obtained by the oscillating electrons, metal nanoparticles turn into nano-sources of heat [70, 71]. The latter diffuses away from the lattice via phonon–phonon relaxation, leading to temperature elevation of the surrounding medium which can be exploited to trigger drug payload release [72–80] and/or the thermal destruction of cancer cells (photothermal therapy, PTT) [81–91].

Owing to their high atomic number, AuNPs have a strong X-ray absorption cross-section, making them effective radiosensitizers for enhanced radiotherapy (RT) [92] and efficient contrast agents for X-ray computed tomography imaging [51, 52]. Finally, due to their aforementioned light absorption/scattering properties, AuNPs have been extensively investigated as promising contrast agents for photoacoustic and light scattering imaging techniques [93–95]. These properties—integrated into a single platform—highlight the great potential of AuNPs in light-mediated cancer theranostics [91] and combinatorial cancer therapy [51], providing the unique opportunity to combine simultaneously various diagnosis and treatment modalities with final synergistic effects and enhanced therapeutic outcome.

The combination of the appealing properties of TMCs and AuNPs is now attracting great attention in the scientific community focused on cancer theranostics. An excellent review has recently summarized progress thus far in the nascent field of TMC/AuNP hybrids, focusing particularly on the synthetic protocols, on the multiple characterization techniques as well as on the potential application in imaging, photodynamic therapy, nonlinear optics and catalysis [96]. Herein, we focus our attention on TMCs—in particular ruthenium, iridium and platinum complexes—that have been in the last five years successfully employed in combination with gold nanostructures for in-vitro/in-vivo cancer photo-theranostics.

2 A winning combination: transition metal complexes@gold nanoparticles (TMC@AuNPs)

To date several studies have been reported concerning the photophysical properties of TMCs attached to AuNPs surface or placed at fixed distances from it [97–102]. Depending on the distance, nanoparticle size/shape and extent of the spectral overlap between the TMCs emission band and AuNPs plasmonic band, energy and/or electron transfer processes can take place in TMC@AuNP hybrids, resulting in a quenching of the TMCs radiative deactivation [97–101]. On the contrary, in other cases, an enhancement of the TMCs absorption cross-section [103] or luminescence intensity [102] has been observed.

In this section, we will discuss the most relevant aspects regarding the in-vitro/in-vivo applications of TMC@AuNPs in cancer photo-diagnosis and/or photo-treatment from

2014 to date. We will start focusing on their use in imaging techniques and then in phototherapy treatments, in particular PDT and PTT. Then, their application in chemotherapy and in dual- and triple-modality cancer therapies will be described. All discussed TMC@AuNP systems and related application details are reported in Table 1.

2.1 Imaging in-vitro/in-vivo

The first example of Ru(II) polypyridyl functionalized AuNPs as useful cellular imaging probes was reported by Elmes et al. [121]. The successful combination of AuNPs labelled with a luminescent Ru(II) polypyridyl complex was later explored by Rogers and coworkers [104], reporting an efficient coating method for water soluble AuNPs by using a non-ionic fluorinated surfactant (Zonyl 7950). The selected Ru(II) complex bears two thiol groups to bind the AuNPs surface and a hexyl spacer to distance the ruthenium center from the gold core. The obtained nanospheres Ru(II)@AuNPs – with a diameter of 13 and 100 nm – respectively with 10^3 and 10^5 Ru(II) complex molecules per AuNP—are red-emissive with an enhanced luminescence lifetime compared to TMC free molecule. Their potential in cellular imaging was highlighted in A549 human lung cancer cells by using conventional optical microscopy techniques. In particular, due to the strong scattering signal of the gold core, Ru(II)@AuNPs appear as bright spots in the confocal reflection images, whereas confocal luminescence displays the intense emission of the TMC molecules upon excitation at 453 nm. Striking, Ru(II)@AuNPs with a size of 100 nm, have been clear imaged in tumor cells at a single nanoparticle resolution.

A fluorinated surfactant and an Ir(III) complex (IrC6)—bearing 2-(hexylphenyl)-pyridine as cyclometalated ligands and a bipyridine with long legs as ancillary ligand—(Scheme 1 from Ref. [103]) have been used to coat water-soluble 13, 25, and 100 nm-diameter gold nanospheres (AuNP13, AuNP25, and AuNP100) in order to develop novel nanoprobes for two-photon lifetime imaging in cancer cells [103]. The different lifetime range—hundreds of nanoseconds for the Ir(III) complex, tens of picoseconds for the AuNPs—allowed a two-channel detection of IrC6@AuNP in live HeLa cells, monitoring independently the gold scaffold and the TMC signal. The presence of the gold nanostructure led to an increased two-photon absorption cross section in IrC6@AuNP25 with respect to the IrC6 molecule. Noteworthy, taking advantage of the Ir(III) complex luminescence lifetime sensitivity to the cell

Table 1 TMC@AuNP application in cancer photo-theranostics

Application	Test	Metal center of the TMC	AuNP shape (size/nm)	Cell line/Tumor model	References
Imaging	in-vitro	Ru(II)	sphere (13, 100)	A549	[104]
Imaging	in-vitro	Ir(III)	sphere (13, 25, 100)	HeLa	[103]
Imaging	in-vitro /in-vivo	Ir(III)	sphere (10)	HeLa	[105]
PDT/Imaging	in-vitro	Ru(II)	sphere (5)	TS/A-pc	[106]
PTT/Imaging	in-vitro /in-vivo	Ru(II)	sphere (45)	HeLa	[107]
PTT/Imaging	in-vitro /in-vivo	Ru(II)	rod (40 × 13), star (sphere 20, tips 15–25)	HeLa	[108]
PDT/PTT/Imaging	in-vitro	Ir(III)	sphere (5)	U87MG	[109]
PTT/Chemotherapy	in-vitro	Pt(II)	hollow sphere (43.9, thickness 3–4)	KB	[110]
PTT/Chemotherapy	in-vitro /in-vivo	Pt(II)	hollow sphere (85.6)	HeLa	[111]
PTT/Chemotherapy	in-vitro /in-vivo	Pt(II)	rod (~ 50 × 10)	4T1	[112]
PTT/Chemotherapy	in-vitro /in-vivo	Pt(II)	rod (~ 80 × 15)	4T1	[113]
PTT/Chemotherapy	in-vitro /in-vivo	Pt(IV)	rod (~38.5 × 9.5)	HeLa	[114]
PTT/Chemotherapy	in-vitro /in-vivo	Pt(IV)	hexagonal Pd@Au nanosheets (~ 30, thickness 4)	QGY-7703, QSG-7701, HeLa, S180	[115]
PTT/Chemotherapy/Imaging	in-vitro /in-vivo	Pt(II)	core–shell sphere (~ 70)	SKOV3	[116]
PTT/Chemotherapy/Dual-modal Imaging	in-vitro /in-vivo	Pt(II)	rod (~ 54 × 15)	H1299	[117]
PTT/Chemotherapy/Tri-modal Imaging	in-vitro /in-vivo	Ir(III)	star (75)	MDA-MB-231	[118]
PDT/PTT/Chemotherapy	in-vitro /in-vivo	Pt(IV)	rod (39.8–10.2)	HepG2	[119]
PTT/Chemotherapy/Radio-therapy	in-vivo	Pt(II)	sphere (~ 40)	CT26	[120]

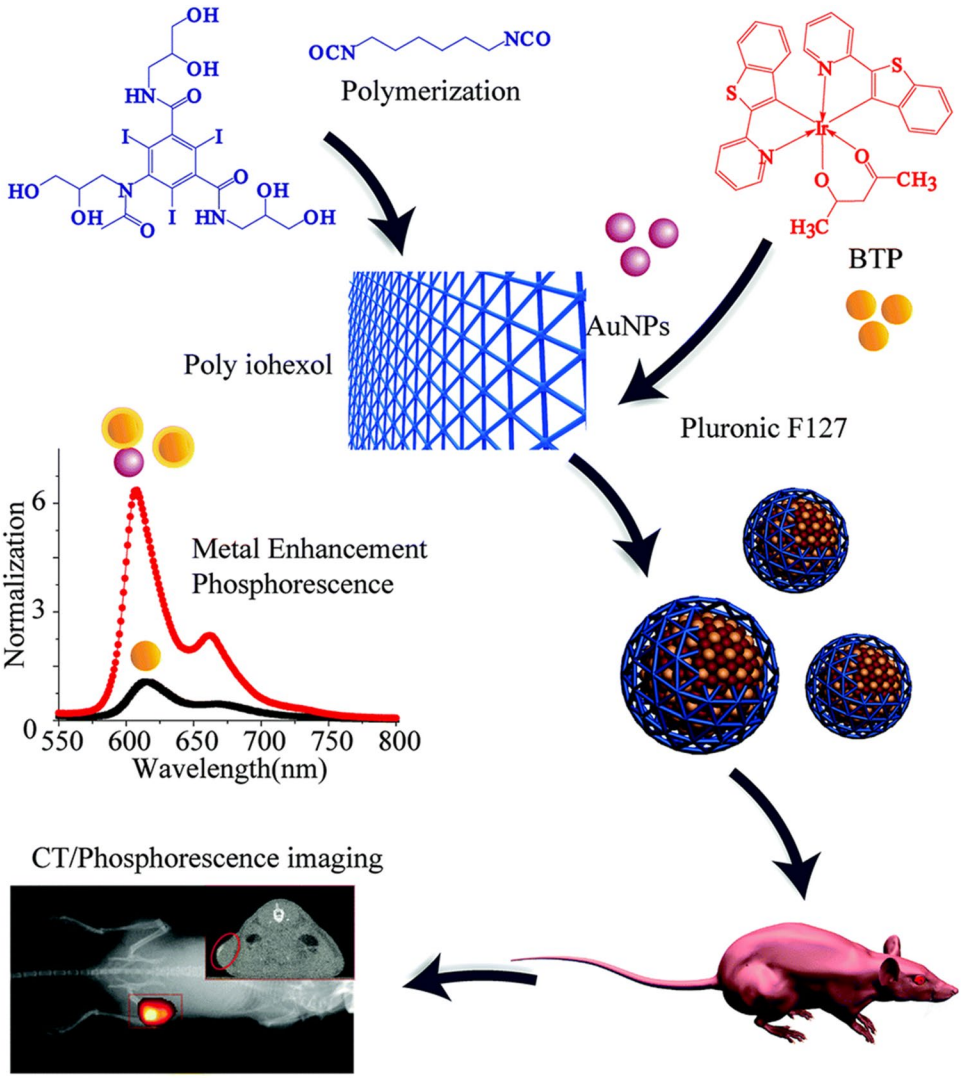

Fig. 1 Schematic representation of the synthesis process of polyiohexol, the fabrication of BAPI NPs and the dual-model imaging of BAPI NPs. Reproduced with permission from Ref [105]. Copyright 2017 Royal Society of Chemistry

environment, with values ranging from 450 to 1000 ns, an IrC6@AuNP intracellular localization map was obtained for all nanoparticle sizes investigated (Fig. 7 from Ref. [103]).

Dual-modal phosphorescence/computed tomography (CT) bioprobes were reported by Yu et al. [105]. In particular, a bis(2-(2′-benzothienyl)pyridinato-N, $C^{3'}$) Ir(III) complex and AuNPs (~ 10 nm-diameter) are both encapsulated within polyiohexol nanoparticles leading to composite nanoparticles (BAPI NPs) with an average size of ~ 50 nm for in-vitro and in-vivo imaging of HeLa cells. AuNPs are used as CT contrast agent and—due to the proximity to the TMC—as metal-enhancement fluorescence effect (MEF) agents, with consequent improvement in phosphorescence imaging (Fig. 1). The average luminescence intensity of the BAPI NPs was 5.85 times higher than that of TMC alone in-vivo. A clear outline of the tumor area after mice injection with BAPI NPs highlighted the excellent CT contrasting ability at low doses. Moreover, since the Ir(III) complex is a hypoxic phosphorescence dye, the tumor showed a distinctly brighter red light than that of other tissues and organs.

2.2 Phototherapy in-vitro/in-vivo

In this section we will focus on the light-activated cancer therapeutic approaches carried out employing TMC@AuNPs nanoplatforms. Initially, we will present treatment modalities based on a single approach or "monotherapy", such as PDT or PTT. Then, we will point out on the unique opportunity to implement an all-in-one TMC@AuNPs formulation—by taking the full advantages of AuNPs and the fascinating properties of TMCs—for combinatorial cancer therapy. Indeed, a new emerging trend in clinical oncology is the combination of two or more treatment modalities—including phototherapies, chemotherapy, radiotherapy – in order to exploit their cooperative interactions,

resulting in a stronger therapeutic efficacy than that observed using separately every single treatment [51].

2.2.1 Monotherapy

2.2.1.1 PDT/imaging As aforementioned, a single TMC molecule can act simultaneously as imaging probe and PDT agent. In this frame, our group presented the new combination Ru(II) polypyridyl complexes/gold silica-based nanoparticles (Ru1@GSNP and Ru2@GSNP), as promising nanomaterial for application in imaging and phototherapy [106]. TMCs—encapsulated in the polysiloxane matrix of 50 nm core–shell nanospheres—displayed singlet oxygen generation ability and luminescence properties in the red region of the electromagnetic spectrum. The light exposure of murine mammary adenocarcinoma (TS/A-pc) cells—after incubation with Ru1@GSNP—triggered a remarkable photodynamic activity of the functionalized nanoparticles and a higher inhibition efficiency of the tumor cells proliferation compared with the TMC alone. Moreover, their intrinsic phosphorescence allowed the localization into the TS/A-pc cytosol by fluorescence microscopy, configuring the nanostructures as multifunctional nanoplatforms for theranostic purposes.

2.2.1.2 PTT/imaging Plasmonic structures at the nanoscale exhibit the renowned ability to transduce the absorbed radiant energy into heat, leading to a local temperature increase. Zhang and coworkers [107] reported an unexpected high photothermal conversion efficiency of gold nanospheres upon grafting with two-photon luminescent Ru(II) polypyridyl complexes. The authors prepared three samples of grafted nanoparticles differed in the distance between the Ru(II) center and the gold surface, and explored how the two-photon luminescence and PTT efficiency changed with the distance. The luminescence was partly quenched due to an energy transfer process from the TMC to the AuNPs depending on the distance from the gold core. The best dual functional nanoparticles of this study was successfully used for real-time luminescent imaging-guided PTT in HeLa cells. The results showed that this sample has a great PTT effect in living cells markedly higher than that of AuNPs, which only displayed a weak PTT effect. Moreover, in-vivo experiments displayed that its use provided tumor ablation under 808 nm irradiation at a low power density. In another paper, the same authors illustrated the results obtained by modifying the shape of the nanoparticles, functionalizing gold nanorods (AuNRs) and gold nanostars (AuNTs) with the most performing Ru(II) complex (Fig. 1a from Ref. [108]). Due to the photothermal effect, naked AuNRs and AuNTs easily melt into gold spheres. This drawback results in loss of the characteristic near-infrared surface plasmon resonance, limiting their therapeutic application. On the contrary, Ru(II) complex-functionalized AuNRs and AuNTs (AuNRs@Ru and AuNTs@Ru, respectively) displayed higher photothermal stability and photothermal conversion efficiency than naked AuNRs and AuNTs. In-vivo PTT studies on HeLa tumor-xenograft mouse model confirmed the different thermal efficiency. After intratumorally injection and laser irradiation for 5 min at 808 nm (Fig. 7 from Ref. [108]), the authors observed a temperature increase of 3, 13, 13, 23.8 and 22.4 °C, for tumor injected respectively with physiological saline, AuNRs, AuNTs, AuNRs@Ru and AuNTs@Ru. Finally, for the experimental groups treated with AuNRs/AuNTs + laser irradiation only a slight delay of tumor growth was observed with respect to the control groups, whereas the groups treated with AuNRs@Ru/AuNTs@Ru + laser irradiation showed photothermal destruction of tumors and no reoccurrence on day 15 (Fig. 9 from Ref. [108]).

2.2.2 Dual-modal therapy

2.2.2.1 PDT/PTT/imaging An example of multimodal synergistic approach was recently presented by our group [109]. A core–shell gold–silica nanoplatform has been engineered for simultaneous cellular imaging, photodynamic and photothermal therapies: a cationic phenylpyridinate Ir(III) complex, spectrally resonant with the gold core, was properly chosen as photosensitizer and luminescent probe and then encapsulated within the polysiloxane matrix. The spectral overlap between the emission band of the cyclometalated complex and the gold plasmon resonance, led to a competitive energy transfer process from the molecule to the AuNP. Then, in the implemented nanosystem, the radiant energy absorbed by the TMC is partly transferred to molecular oxygen—generating singlet oxygen (photodynamic effect)—and partly to the gold core, with consequent conversion into heat (photothermal effect). In-vitro photo-cytotoxicity tests on human glioblastoma cells (U87MG) demonstrated a high cytotoxic ability of the nanoplatform, reducing the cell viability to 10% already at very low doses (1 μM). Moreover, due to the luminescence properties of the TMC, fluorescence imaging was used to determine the cellular uptake and intracellular distribution of nanostructures [109].

2.2.2.2 PTT/chemotherapy Xiong et al. [110] presented a dual therapeutic approach—photothermal therapy and NIR laser-triggered platinum-based chemotherapy—employing hollow gold nanoparticles (HGNPs). They synthesized and characterized cisplatin-loaded HGNPs using a tripeptide, acetyl-Glu-Glu-Cys-NH_2 (Ac-EEC), as both Pt(II)-chelating agent and linker to HGNPs (Fig. 2a). Finally, folic acid (F) molecules—conjugated to the gold

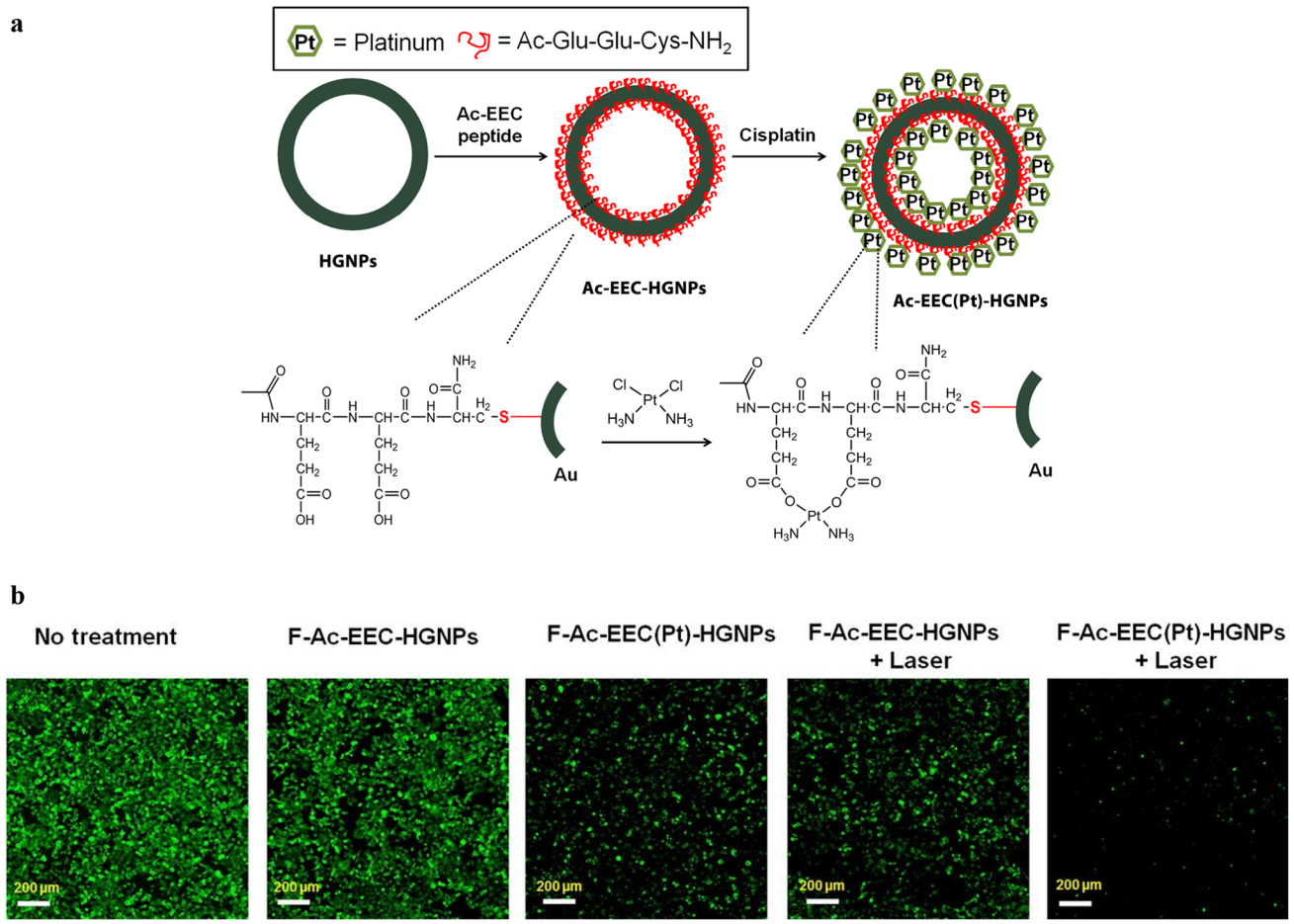

Fig. 2 **a** Schematic illustrations of cisplatin-loaded HGNPs. The HGNPs incorporating cisplatin (Pt) are spontaneously formed via a ligand exchange reaction of Pt(II) from the chloride to the carboxylates in the Ac-EEC peptide in distilled water. **b**, Microphotographs showing enhanced cell killing with combined F-Ac-EEC-HGNPs and laser treatments. KB cells were exposed to F-Ac-EEC-HGNPs without Pt loading or F-Ac-EEC(Pt)-HGNPs with Pt loading for 4 h. The cells were irradiated or not with a pulsed laser at 808 nm (50 mW/cm^2; 1 min). After washing steps and an additional 20 h incubation, cells were stained with calcein AM. Green fluorescence represents viable cells. Bar, 200 µm. Reproduced with permission from Ref [110]. Copyright 2018 Springer Nature

surface—were used as targeting molecules. The resulting F-Ac-EEC(Pt)-HGNPs nano-carrier system was tested in-vitro on folate receptor-expressing KB cells, with and without laser irradiation at 808 nm, corresponding to the plasmon resonance frequency of gold nanostructures. As clearly shown in Fig. 2b, without laser irradiation F-Ac-EEC(Pt)-HGNPs display a cytotoxic effect against cancer cells due to the intracellular release of the cisplatin molecule by an ion-exchange process. The same nanostructures without the Pt(II) complex, F-Ac-EEC-HGNPs, upon NIR laser irradiation induce a reduction of the cell viability due to the plasmonic-mediated photothermal effects. Finally, F-Ac-EEC(Pt)-HGNPs combined with NIR laser irradiation displayed the greatest effects on cell mortality due to the dual approach—photothermal-chemotherapy—resulting in thermal ablation and rapid release of soluble Pt(II) compounds.

A similar combination TMC@AuNP for in-vitro/in-vivo treatment of cervical cancer has been reported by Guan et al. [111]. The tested nanostructures consist of PEG-coated hollow gold nanospheres (HGNs) loaded with cisplatin. Then, NIR laser irradiation was applied to increase the drug penetration into the tumor tissue and improve its delivery, taking advantage of the photothermal conversion properties of HGNs. In-vitro test showed that the combination cisplatin-PEG-HGNs-808 nm irradiation induces a higher cytotoxicity in HeLa cells respect to the non-irradiated system, with a cell viability after treatment respectively of 20% and 60%. Finally, the formulation cisplatin-PEG-HGNs-808 nm light exposure was found to be the most effective in in-vivo studies, leading to a marked tumor regression in mice.

Feng and coworkers [112] described the synthesis and characterization of gold nanorods (GNRs) coated with

thiolated poly(ethylene glycol)-graft-poly(L-glutamic acid) copolymers conjugated with folic acid (FA-GNR). The cytotoxic drug cisplatin was then loaded on FA-GNR via coordination bonds between the carboxylic groups of polypeptide poly(L-glutamic acid) and the platinum atom (FA-GNR@Pt), for targeted photothermal/chemotherapy of triple negative breast cancer (TNBC). The obtained FA-GNR@Pt nanostructures enclose—into one single nanosystem—the photothermal conversion properties of GNRs, the high biocompatibility of poly(L-glutamic acid), the anticancer activity of cisplatin and the tumor targeting ability of folic acid. Relative cell viability of 4T1 cells after incubation with FA-GNR@Pt hybrid nanoparticles and exposed to laser irradiation at 655 nm, was significantly reduced to 10%, whereas the treatment with cisplatin molecules—or with the corresponding nanostructures without the cisplatin component—leads the cell viability to 70% and 30%, respectively, highlighting the higher therapeutic efficiency of the dual chemo-thermal approach compared with the related individual monotherapies. Then, the antitumor efficacy and biosafety of FA-GNR@Pt nanoparticles were evaluated in-vivo on TNBC-bearing mice. In particular, the combination of a systemic administration of FA-GNR@Pt with localized near infrared laser illumination resulted in a complete inhibition of the primary tumor growth and the simultaneous prevention of lung metastasis.

Gao et al. [113] realized a cutting edge dual-drug delivery biomimetic system—based on gold nanorods, doxorubicin and cisplatin—for synergistic chemo-photothermal therapy. The surface of the nanorods was first modified with hyaluronic acid followed by the antitumor drugs incorporation. The obtained nanogel system was cloaked with 4T1 cancer cell membrane in order to improve the interactions with the homotypic cells and thus its targeting ability. The 4T1- hyaluronic acid nanogel—gold nanorod – doxorubicin – cisplatin nanostructure (4T1-HANG-GNR-DC) exhibited a dramatically increased cellular uptake. The high intrinsic photothermal conversion efficiency of the gold nanostructures was used to produced heat and then stimulate the drugs release from the particles after cellular uptake. In-vitro test on 4T1 cells showed that the viability was reduced to less than 6% after incubation with 4T1-HANG-GNR-DC followed by irradiation at 808 nm, a cytotoxic effect higher than that obtained by treating tumor cells only with the chemotherapeutic agents or with the dual-drug delivery system without light exposure. The authors then assessed the in-vivo antitumor efficacy of 4T1-HANG-GNR-DC on mice bearing a 4T1 xenograft mammary tumor; compared with the saline group treatment, the tumor volume was suppressed by 96% after intravenous injection of 4T1-HANG-GNR-DC followed by NIR irradiation.

Shanmugam and colleagues [114] reported a light-responsive dual drugs delivery system—based on gold nanorods (AuNRs) and DNA duplexes—for in-vitro/in-vivo cancer photothermal ablation and combination chemotherapy. In particular, the double stranded DNA—tethered to the AuNRs surface—was loaded with doxorubicin and the Pt(IV) prodrug *c,c,t*-$Pt(NH_3)_2Cl_2(OOCCH_2CH_2COOH)_2$, the latter in turn conjugated with folic acid by amide binding in order to improve the nanoplatform targeting ability towards cancer cells. It is generally known that Pt(IV) complexes with a high coordination number are kinetically inert and therefore result in fewer side effects compared with Pt(II) species [122, 123]. The NIR-laser irradiation of the developed nanosystem provided hyperthermia and induced the dehybridization of the duplex DNA with consequent chemotherapeutic drugs release. Then, the Pt(IV) prodrugs—inside the cancer cells—were reduced by physiological reductants (e.g. ascorbic acid or glutathione) into their cytotoxic and hydrophilic Pt(II) derivative. In-vitro studies on HeLa cells showed significant cell toxicity after incubation with the nanoplatform followed by irradiation at 808 nm and in-vivo experiments on xenografted mouse tumor model confirmed its therapeutic efficacy.

Shi et al. [115] successfully conjugated PEGylated core–shell Pd@Au nanoplates with the same above-mentioned Pt(IV) prodrug *c,c,t*-$Pt(NH_3)_2Cl_2(OOCCH_2CH_2COOH)_2$, obtaining a nanocomposite (Pd@Au-PEG-Pt) for combined photothermal-chemotherapy. Core–shell Pd@Au nanoplates consist of ultrathin palladium nanosheets on whose surface, gold was successfully grown. The obtained bimetallic nanostructures displayed an intense surface plasmon resonance peak in the NIR region, making them excellent photothermal agents. The NIR irradiation not only enables Pd@Au-PEG-Pt to generate heat for killing cancer cells, but also promotes the release and the chemical reduction of the Pt(IV) prodrug by the bio-reductant ascorbic acid. In in-vitro experiments, Pd@Au-PEG-Pt under irradiation at 808 nm exhibited a higher cytotoxicity on HeLa, QGY-7703 and QSG-7701 cell lines compared with cisplatin. The photo-treatment of mice bearing S180 tumors after Pd@Au-PEG injection resulted in a complete tumor tissue destruction without recurrence, highlighting that—compared with PTT or chemotherapy alone—combined photothermal-chemotherapy displayed a synergistic effect in improving the therapeutic outcome.

2.2.2.3 PTT/chemotherapy/imaging Zhang et al. [116] synthesized cisplatin-loaded gap-enhanced Raman tags (C-GERTs) for intraoperative real-time Raman detection and chemo-photothermal therapy of disseminated ovarian microtumors. C-GERTs consists of a gold core and a thin gold shell separated by and internal sub-nanometer gap containing 1,4-benzenedithiol Raman

reporters, and an external mesoporous silica layer, with cisplatin molecules loaded into the pores (Scheme 1 from Ref. [116]). The developed nanosystem showed numerous advantages: 1) photothermal properties; 2) "fingerprint" Raman signal from the molecules inside the nanogaps, strongly enhanced by the presence of the gold core–shell nanostructure; 3) biocompatibility of the external silica layer, additionally loaded with a chemotherapeutic drug. In-vitro studies on SKOV3 cells revealed that after treatment with C-GERTs + laser irradiation at 808 nm, almost 100% of tumor cells were killed by chemo-photothermal synergistic therapy. Moreover, the authors reported in-vivo intraoperative real-time Raman detection and treatment of disseminated ovarian microtumors. Mice—24 h after C-GERTs injection—underwent aseptic laparotomy surgery and Raman signals of C-GERTs at 1055 and 1555 cm^{-1} were instantly and easily detected from various tumor size (0.1–0.7 cm in diameter) (Fig. 3a–3c from Ref. [116]). Then, they performed real-time photothermal therapy on the positive Raman locations. In-vivo therapeutic effects after intraoperative chemo-photothermal treatment with multifunctional C-GERTs, showed a near complete elimination of tumors and suppression of regrowth, with a survival rate in SKOV3 mice of 100% during the observation period (Fig. 5e from Ref. [116]).

Another example of image-guided combined chemo-thermal therapy was reported by Zhang et al. [117]. The authors developed a theranostic platform (RGD-IPt-PDA@GNRs) based on polydopamine (PDA)-coated gold nanorods (GNRs), loaded with the anticancer drug cisplatin and labeled with the radioisotope iodine-125. Arginine-glycine-aspartic acid (RGD) peptide was conjugated on the GNRs surface to specifically target tumor angiogenic vessels. Chemo-photothermal therapy effects were evaluated in-vitro on H1299 cells after incubation with RGD-IPt-PDA@GNRs followed by light exposure at 808 nm, revealing a strong decrease in cell viabilities. Then, tumor-bearing mice were injected intravenously with the nanoplatform and single photon emission computed tomography and high-resolution photoacoustic imaging were used to detect RGD-IPt-PDA@GNRs tumor accumulation and angiogenic vessels, confirming that RGD-IPt-PDA@GNRs specifically addressed the latter. Finally, in-vivo studies displayed chemo-photothermal synergistic therapeutic effect on H1299 bearing mice, leading to tumor ablation without relapse.

Yu et al. [118] presented the first example of a combination Ir(III) complex/gold nanomaterials for TNBC multimodal imaging and synergistic photothermal-chemotherapy. The anticancer $[Ir(thp)_2phen]^+PF_6^-$ compound was loaded on gold nanostars (GNS) (Fig. 3a), that due to their branched structure exhibited a plasmonic resonance peak at 808 nm and consequent photothermal conversion ability in the NIR region. In order to enhance the targeting ability against the urokinase-type plasminogen activator receptor overexpressed by malignant cancer cells, the GNS@Ir nanoplatform was functionalized with polyetherimide-AE105 peptide conjugate (Fig. 3a). The resultant GNS@Ir@P-AE105 nanostructure showed an efficient MDA-MB-231 cell uptake and selectivity, a NIR laser controlled release of the TMC, an excellent photothermal/photoacoustic/X-ray computed tomography imaging ability and a synergistic photothermal and chemotherapeutic effect on MDA-MB-231 cells (Fig. 3b). In particular, the IC_{50} of GNS@Ir@P-AE105 reduced about 10 times compared with that of the Ir(III) complex or GNS used individually, whereas the in-vivo investigation on MDA-MB-231 tumor-bearing mice—after intratumoral injection of GNS@Ir@P-AE105 followed by NIR laser irradiation—revealed an almost complete tumor regression.

2.2.3 Tri-modal therapy

2.2.3.1 PDT/PTT/chemotherapy Luo and coworkers [119] developed a highly integrated nanocomposite based on mesoporous silica-coated gold nanorods (MSGNR) for tri-synergistic tumor therapy. The photosensitizer Al(III) phthalocyanine chloride tetrasulfonic acid ($AlPcS_4$) was loaded within the porous structure of the silica shell. The polysiloxane surface was functionalized with β-cyclodextrin (β-CD) molecules used as "gatekeepers" to block the premature release of entrapped $AlPcS_4$ and immobilized on MSGNR via a redox-cleavable Pt(IV) complex—derivative of cisplatin—leading to a redox-responsive drug delivery system. In particular, the linker Pt(IV) prodrug *c,c,t*-$Pt(NH_3)_2Cl_2(OOCCH_2CH_2COOH)_2$ is conjugated to the amine groups of MSGNR-NH_2 and mono-6-ethylenediamine-β-CD by amide bonds. Finally, adamantane (Ad) conjugated poly(ethylene glycol) (Ad-PEG) and lactobionic acid (Ad-LA) were linked on the β-CD through host–guest interaction to promote long term circulation and tumor targeting, respectively. The obtained nanocomposite exhibited very efficient tumor cell selectivity and responsiveness to the intracellular reducing environment triggering the drugs release ($AlPcS_4$ and cisplatin). Under dual light irradiation (808 and 660 nm), the high photothermal conversion—intrinsic to gold nanostructures—and ROS (*i.e.* Reactive Oxygen Species) generation—due to the photosensitizer activation—led to remarkable HepG2 cancer cells death with only 8% cells survival, strongly highlighting the advantage of the triple-combination therapy. In-vivo experiments carried out on HepG2 tumor-bearing nude mice also revealed the improved tumor accumulation of the nanosystem as well

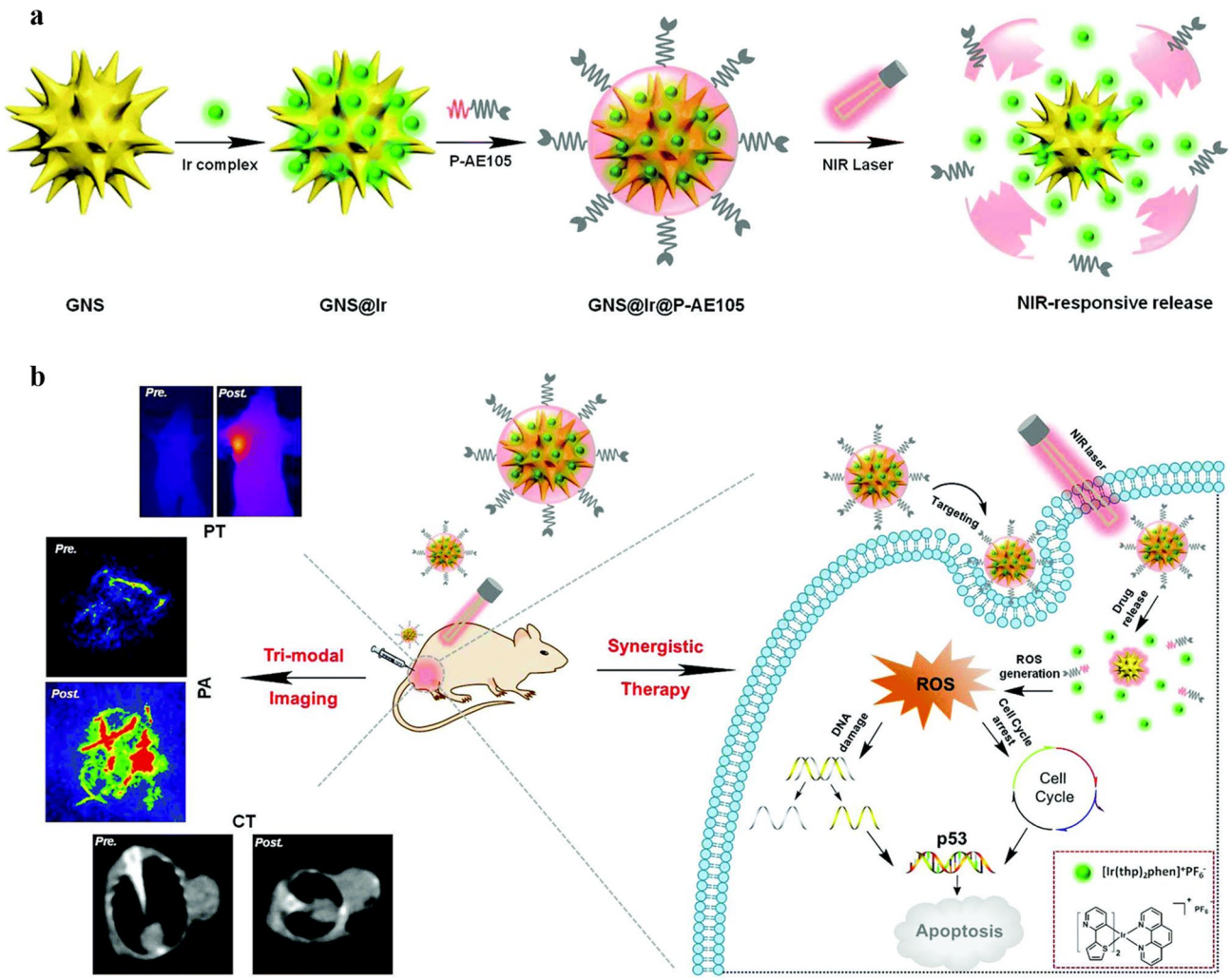

Fig. 3 **a** Schematic illustration of the GNS@Ir@P-AE105 multifunctional nanoplatform preparation and **b**, its application for multimodal imaging and synergistic photothermal-chemotherapy of TNBC. Reproduced with permission from Ref. [118]. Copyright 2020 Royal Society of Chemistry

as the higher tumor growth inhibition compared to other treatments groups.

2.2.3.2 PTT/chemotherapy/radiotherapy A multimodal synergistic cancer therapy approach has also been reported by Mirrahimi et al. [120]. The authors developed a thermo-responsive and radiosensitizing nanoplatform (ACA) by incorporating gold nanospheres and cisplatin into alginate hydrogel to combine chemotherapy, radiotherapy and photothermal therapy. Alginate was used as polymeric carrier for delivery of AuNPs and cisplatin, where gold nanostructures were employed for enhanced radiotherapy and laser-induced photothermal therapy. The antitumor activity of ACA—upon irradiation at 532 nm and 6 MV X-ray—was evaluated in-vivo on murine CT26 colon adenocarcinoma model. Compared to dual-therapy treatment groups—thermo-chemo therapy (ACA + laser)—chemoradiation (ACA + RT)—and thermo-radio therapy (alginate coated AuNPs + laser + RT), trimodal thermo-chemo-radio therapy (ACA + laser + RT) exhibited the most pronounced antitumor efficiency, with a complete tumor eradication and no evidence of relapse during the 90-days follow up period.

3 Conclusions

In this review, we summarized the recent advances in cancer photo-theranostics by using the hybrid combination transition metal complexes/gold nanoparticles as light-triggered therapeutic/diagnostic agents. The main objective was to highlight—going through the several examples reported—the emerging role of TMC@AuNPs nanomaterials in the cutting-edge field of simultaneous

diagnosis and therapy of cancer, providing the opportunity to easily tune their properties by properly coupling plasmonic AuNPs—of a specific shape/size—with TMCs having a particular metal center and/or ligands. Certainly, the strength of both components—TMCs and AuNPs—is their ability to interact with the Vis–NIR light radiation, resulting in exclusively light-mediated and then highly localized treatments. As well, the tumor-selective approach can further improved by functionalizing the nanostructures surface with ligand motifs to specifically target cancer cells. The hybrid combination provides the unique opportunity to confine in a single nanostructure a wide range of treatment strategies—i.e. chemotherapy, radiotherapy, photodynamic/photothermal therapies—and to exploit the cooperative interactions between them, resulting in a stronger efficacy than that observed using separately every single therapeutic approach. Cisplatin derivatives and Pt(IV) pro-drugs are well known as chemotherapeutic agents and combined with light-responsive AuNPs can lead to efficient photo-induced drug delivery systems with synergistic therapeutic effects; Ir(III) and Ru(II) complexes exhibit electronic excited states with an energy suitable to promote efficient energy transfer processes towards molecular oxygen and/or plasmonic AuNPs, resulting in photodynamic and photothermal effects. Finally, the intrinsic luminescence of TMCs provides the opportunity to use TMC@AuNPs nanosystems also in fluorescence bioimaging, whereas the presence of AuNPs makes them efficient contrast agents for X-ray computed tomography, photoacoustic and light scattering imaging techniques. Based on the multifaceted advantages, we can certainly expect that the winning combination transition metal complexes/gold nanoparticles will be widely explored in the near future affording significant opportunities in the cancer theranostics field.

Compliance with ethical standards

Conflict of interest The authors declare that there is no conflict of interest.

References

1. Ko C-N, Li G, Leung C-H, Ma D-L (2019) Dual function luminescent transition metal complexes for cancer theranostics: The combination of diagnosis and therapy. Coord Chem Rev 381:79–103. https://doi.org/10.1016/j.ccr.2018.11.013
2. Sodhi RK, Paul S (2019) Metal complexes in medicine: An overview and update from drug design perspective. Canc Therapy Oncol Int J 14:555883. https://doi.org/10.19080/CTOIJ.2019.13.555883
3. Rosenberg B, Van Camp L, Krigas T (1965) Inhibition of cell division in *Escherichia Coli* by electrolysis products from a platinum electrode. Nature 205:698–699. https://doi.org/10.1038/205698a0
4. Kelland L (2007) The resurgence of platinum-based cancer chemotherapy. Nat Rev Cancer 7:573–584. https://doi.org/10.1038/nrc2167
5. Harrap KR (1985) Preclinical studies identifying carboplatin as a viable cisplatin alternative. Cancer Treat Rev 12:21–33. https://doi.org/10.1016/0305-7372(85)90015-5
6. Kidani Y, Inagaki K, Iigo M, Hoshi A, Kuretani K (1978) Antitumor activity of 1,2-Diaminocyclohexane-platinum complexes against Sarcoma-180 Ascites form. J Med Chem 21:1315–1318. https://doi.org/10.1021/jm00210a029
7. Kelland LR, Abel G, McKeage MJ, Jones M, Goddard PM, Valenti M, Murrer BA, Harrap KR (1993) Preclinical antitumor evaluation of Bis-acetato-ammine-dichloro-cyclohexylamine Platinum(IV): an orally active platinum drug. Cancer Res 53:2581–2586
8. Holford J, Sharp SY, Murrer BA, Abrams M, Kelland LR (1998) In vitro circumvention of cisplatin resistance by the novel sterically hindered platinum complex AMD473. Br J Cancer 77:366–373. https://doi.org/10.1038/bjc.1998.59
9. Zhao Q, Huang C, Li F (2011) Phosphorescent heavy-metal complexes for bioimaging. Chem Soc Rev 40:2508–2524. https://doi.org/10.1039/c0cs00114g
10. Guan R, Xie L, Rees TW, Ji L, Chao H (2020) Metal complexes for mitochondrial bioimaging. J Inorg Biochem 204:110985. https://doi.org/10.1016/j.jinorgbio.2019.110985
11. Chen Y, Guan R, Zhang C, Huang J, Ji L, Chao H (2016) Two-photon luminescent metal complexes for bioimaging and cancer phototherapy. Coord Chem Rev 310:16–40. https://doi.org/10.1016/j.ccr.2015.09.010
12. Baggaley E, Weinstein JA, Williams JAG (2012) Lighting the way to see inside the live cell with luminescent transition metal complexes. Coord Chem Rev 256:1762–1785. https://doi.org/10.1016/j.ccr.2012.03.018
13. Zhen X, Qu R, Chen W, Wu W, Jiang X (2020) The development of phosphorescent probes for in vitro and in vivo bioimaging. Sci, Biomater. https://doi.org/10.1039/d0bm00819b
14. Shum J, Leung PK-K, Lo KK-W (2019) Luminescent Ruthenium(II) polypyridine complexes for a wide variety of biomolecular and cellular applications. Inorg Chem 58:2231–2247. https://doi.org/10.1021/acs.inorgchem.8b02979
15. Tang TS-M, Yip AM-H, Zhang KY, Liu H-W, Wu PL, Li KF, Cheah KW, Lo KK-W (2015) Bioorthogonal labeling, bioimaging, and photocytotoxicity studies of phosphorescent Ruthenium(ii) polypyridine dibenzocyclooctyne complexes. Chem - A Eur J 21:10729–10740. https://doi.org/10.1002/chem.201501040
16. Neugebauer U, Pellegrin Y, Devocelle M, Forster RJ, Signac W, Moran N, Keyes TE (2008) Ruthenium polypyridyl peptide conjugates: Membrane permeable probes for cellular imaging. Chem. Commun. pp. 5307–5309https://doi.org/10.1039/b810403d
17. Gill MR, Garcia-Lara J, Foster SJ, Smythe C, Battaglia G, Thomas JA (2009) A ruthenium(II) polypyridyl complex for direct

imaging of DNA structure in living cells. Nat Chem 1:662–667. https://doi.org/10.1038/nchem.406
18. Baggaley E, Gill MR, Green NH, Turton D, Sazanovich IV, Botchway SW, Smythe C, Haycock JW, Weinstein JA, Thomas JA (2014) Dinuclear ruthenium(II) complexes as two-photon, time-resolved emission microscopy probes for cellular DNA. Angew Chemie - Int Ed 53:3367–3371. https://doi.org/10.1002/anie.201309427
19. Martí AA, Puckett CA, Dyer J, Stevens N, Jockusch S, Ju J, Barton JK, Turro NJ (2007) Inorganic-organic hybrid luminescent binary probe for DNA detection based on spin-forbidden resonance energy transfer. J Am Chem Soc 129:8680–8681. https://doi.org/10.1021/ja0717257
20. Martin A, Byrne A, Burke CS, Forster RJ, Keyes TE (2014) Peptide-bridged dinuclear Ru(II) complex for mitochondrial targeted monitoring of dynamic changes to oxygen concentration and ROS generation in live mammalian cells. J Am Chem Soc 136:15300–15309. https://doi.org/10.1021/ja508043q
21. Caporale C, Massi M (2018) Cyclometalated iridium(III) complexes for life science. Coord Chem Rev 363:71–91. https://doi.org/10.1016/j.ccr.2018.02.006
22. Shaikh S, Wang Y, ur Rehman F, Jiang H, Wang X, (2020) Phosphorescent Ir (III) complexes as cellular staining agents for biomedical molecular imaging. Coord Chem Rev 416:213344. https://doi.org/10.1016/j.ccr.2020.213344
23. Ho P-Y, Ho C-L, Wong W-Y (2020) Recent advances of iridium(III) metallophosphors for health-related applications. Coord Chem Rev 413:213267. https://doi.org/10.1016/j.ccr.2020.213267
24. Lee LC-C, Tsang AW-Y, Liu H-W, Lo KK-W (2020) Photofunctional cyclometalated Iridium(III) polypyridine complexes bearing a perfluorobiphenyl moiety for bioconjugation, bioimaging, and phototherapeutic applications. Inorg Chem 59:14796–14806. https://doi.org/10.1021/acs.inorgchem.0c01343
25. Shi H, Sun H, Yang H, Liu S, Jenkins G, Feng W, Li F, Zhao Q, Liu B, Huang W (2013) Cationic polyfluorenes with phosphorescent iridium(III) complexes for time-resolved luminescent biosensing and fluorescence lifetime imaging. Adv Funct Mater 23:3268–3276. https://doi.org/10.1002/adfm.201202385
26. Li C, Yu M, Sun Y, Wu Y, Huang C, Li F (2011) A nonemissive iridium(III) complex that specifically lights-up the nuclei of living cells. J Am Chem Soc 133:11231–11239. https://doi.org/10.1021/ja202344c
27. He L, Tan C-P, Ye R-R, Zhao Y-Z, Liu Y-H, Zhao Q, Ji L-N, Mao Z-W (2014) Theranostic iridium(III) complexes as one- and two-photon phosphorescent trackers to monitor autophagic lysosomes. Angew Chemie - Int Ed 53:12137–12141. https://doi.org/10.1002/anie.201407468
28. You Y (2013) Phosphorescence bioimaging using cyclometalated Ir(III) complexes. Curr Opin Chem Biol 17:699–707. https://doi.org/10.1016/j.cbpa.2013.05.023
29. Liu S, Liang H, Zhang KY, Zhao Q, Zhou X, Xu W, Huang W (2015) A multifunctional phosphorescent iridium(iii) complex for specific nucleus staining and hypoxia monitoring. Chem Commun 51:7943–7946. https://doi.org/10.1039/c5cc01978h
30. Mauro M, Aliprandi A, Septiadi D, Kehr NS, De Cola L (2014) When self-assembly meets biology: Luminescent platinum complexes for imaging applications. Chem Soc Rev 43:4144–4166. https://doi.org/10.1039/c3cs60453e
31. Li J, Ma Y, Liu S, Mao Z, Chi Z, Qian P-C, Wong W-Y (2020) Soft salts based on platinum(II) complexes with high emission quantum efficiencies in the near infrared region for in vivo imaging. Chem Commun 56:11681–11684. https://doi.org/10.1039/d0cc05366j
32. Ionescu A, Ricciardi L (2017) Water-induced red luminescence in ionic square-planar cyclometalated platinum(II) complexes. Inorganica Chim Acta 460:165–170. https://doi.org/10.1016/j.ica.2016.07.040
33. Chao H, Ouyang C, Li Y, Rees TW, Liao X, Jia J, Chen Y, Zhang X, Ji L (2020) Supramolecular assembly of an organoplatinum(II) complex with ratiometric dual emission for two-photon bioimaging. Angew. Chemie Int. Ed. doi: https://doi.org/10.1002/anie.202014043.
34. Botchway SW, Charnley M, Haycock JW, Parker AW, Rochester DL, Weinstein JA, Williams JAG (2008) Time-resolved and two-photon emission imaging microscopy of live cells with inert platinum complexes. Proc Natl Acad Sci U S A 105:16071–16076. https://doi.org/10.1073/pnas.0804071105
35. Baggaley E, Botchway SW, Haycock JW, Morris H, Sazanovich IV, Williams JAG, Weinstein JA (2014) Long-lived metal complexes open up microsecond lifetime imaging microscopy under multiphoton excitation: From FLIM to PLIM and beyond. Chem Sci 5:879–886. https://doi.org/10.1039/c3sc51875b
36. Li J, Chen T (2020) Transition metal complexes as photosensitizers for integrated cancer theranostic applications. Coord Chem Rev 418:213355. https://doi.org/10.1016/j.ccr.2020.213355
37. Knoll JD, Turro C (2015) Control and utilization of ruthenium and rhodium metal complex excited states for photoactivated cancer therapy. Coord Chem Rev 282–283:110–126. https://doi.org/10.1016/j.ccr.2014.05.018
38. McKenzie LK, Bryant HE, Weinstein JA (2019) Transition metal complexes as photosensitisers in one- and two-photon photodynamic therapy. Coord Chem Rev 379:2–29. https://doi.org/10.1016/j.ccr.2018.03.020
39. Ricciardi L, Puoci F, Cirillo G, La Deda M (2012) A new member of the oxygen-photosensitizers family: A water-soluble polymer binding a platinum complex. Dalt Trans 41:10923–10925. https://doi.org/10.1039/c2dt31157g
40. Zamora A, Vigueras G, Rodríguez V, Santana MD, Ruiz J (2018) Cyclometalated iridium(III) luminescent complexes in therapy and phototherapy. Coord Chem Rev 360:34–76. https://doi.org/10.1016/j.ccr.2018.01.010
41. Karges J, Kuang S, Maschietto F, Blacque O, Ciofini I, Chao H, Gasser G (2020) Rationally designed ruthenium complexes for 1- and 2-photon photodynamic therapy. Nat Commun 11:3262. https://doi.org/10.1038/s41467-020-16993-0
42. Huang H, Banerjee S, Sadler PJ (2018) Recent advances in the design of targeted iridium(III) photosensitizers for photodynamic therapy. ChemBioChem 19:1574–1589. https://doi.org/10.1002/cbic.201800182
43. Imberti C, Zhang P, Huang H, Sadler PJ (2020) New designs for phototherapeutic transition metal complexes. Angew Chemie 132:61–73. https://doi.org/10.1002/ange.201905171
44. Liu J, Zhang C, Rees TW, Ke L, Ji L, Chao H (2018) Harnessing ruthenium(II) as photodynamic agents: Encouraging advances in cancer therapy. Coord Chem Rev 363:17–28. https://doi.org/10.1016/j.ccr.2018.03.002
45. Lemercier G, Four M, Chevreux S (2018) Two-photon absorption properties of 1,10-phenanthroline-based Ru(II) complexes and related functionalized nanoparticles for potential application in two-photon excitation photodynamic therapy and optical power limiting. Coord Chem Rev 368:1–12. https://doi.org/10.1016/j.ccr.2018.03.019
46. Monro S, Colón KL, Yin H, Roque J, Konda P, Gujar S, Thummel RP, Lilge L, Cameron CG, McFarland SA (2019) Transition metal complexes and photodynamic therapy from a tumor-centered approach: challenges, opportunities, and highlights from the development of TLD1433. Chem Rev 119:797–828. https://doi.org/10.1021/acs.chemrev.8b00211
47. Wang X, Wang X, Jin S, Muhammad N, Guo Z (2019) Stimuli-responsive therapeutic metallodrugs. Chem Rev 119:1138–1192. https://doi.org/10.1021/acs.chemrev.8b00209

48. Wong XY, Sena-Torralba A, Álvarez-Diduk R, Muthoosamy K, Merkoçi A (2020) Nanomaterials for nanotheranostics: Tuning their properties according to disease needs. ACS Nano 14:2585–2627. https://doi.org/10.1021/acsnano.9b08133
49. Cheng L, Wang C, Feng L, Yang K, Liu Z (2014) Functional nanomaterials for phototherapies of cancer. Chem Rev 114:10869–10939. https://doi.org/10.1021/cr400532z
50. Lucky SS, Soo KC, Zhang Y (2015) Nanoparticles in photodynamic therapy. Chem Rev 115:1990–2042. https://doi.org/10.1021/cr5004198
51. Beik J, Khateri M, Khosravi Z, Kamrava SK, Kooranifar S, Ghaznavi H, Shakeri-Zadeh A (2019) Gold nanoparticles in combinatorial cancer therapy strategies. Coord Chem Rev 387:299–324. https://doi.org/10.1016/j.ccr.2019.02.025
52. Yang X, Yang M, Pang B, Vara M, Xia Y (2015) Gold nanomaterials at work in biomedicine. Chem Rev 115:10410–10488. https://doi.org/10.1021/acs.chemrev.5b00193
53. Dreaden EC, Alkilany AM, Huang X, Murphy CJ, El-Sayed MA (2012) The golden age: Gold nanoparticles for biomedicine. Chem Soc Rev 41:2740–2779. https://doi.org/10.1039/c1cs15237h
54. Kalyane D, Raval N, Maheshwari R, Tambe V, Kalia K, Tekade RK (2019) Employment of enhanced permeability and retention effect (EPR): Nanoparticle-based precision tools for targeting of therapeutic and diagnostic agent in cancer. Mater Sci Eng C 98:1252–1276. https://doi.org/10.1016/j.msec.2019.01.066
55. Shi J, Kantoff PW, Wooster R, Farokhzad OC (2017) Cancer nanomedicine: Progress, challenges and opportunities. Nat Rev Cancer 17:20–37. https://doi.org/10.1038/nrc.2016.108
56. Maeda H, Wu J, Sawa T, Matsumura Y, Hori K (2000) Tumor vascular permeability and the EPR effect in macromolecular therapeutics: a review. J Control Release 65:271–284. https://doi.org/10.1016/S0168-3659(99)00248-5
57. Ghosh P, Han G, De M, Kim CK, Rotello VM (2008) Gold nanoparticles in delivery applications. Adv Drug Deliv Rev 60:1307–1315. https://doi.org/10.1016/j.addr.2008.03.016
58. Kreibig U, Vollmer M (1995) Optical properties of metal clusters. Springer, Berlin, Heidelberg. https://doi.org/10.1007/978-3-662-09109-8
59. Hu M, Chen J, Li Z-Y, Au L, Hartland GV, Li X, Marquez M, Xia Y (2006) Gold nanostructures: Engineering their plasmonic properties for biomedical applications. Chem Soc Rev 35:1084–1094. https://doi.org/10.1039/b517615h
60. Yang L, Zhou Z, Song J, Chen X (2019) Anisotropic nanomaterials for shape-dependent physicochemical and biomedical applications. Chem Soc Rev 48:5140–5176. https://doi.org/10.1039/c9cs00011a
61. Averitt RD, Westcott SL, Halas NJ (1999) Linear optical properties of gold nanoshells. J Opt Soc Am B 16:1824–1832. https://doi.org/10.1364/JOSAB.16.001824
62. Hong S, Shuford KL, Park S (2011) Shape transformation of gold nanoplates and their surface plasmon characterization: Triangular to hexagonal nanoplates. Chem Mater 23:2011–2013. https://doi.org/10.1021/cm103273c
63. Pérez-Juste J, Pastoriza-Santos I, Liz-Marzán LM, Mulvaney P (2005) Gold nanorods: Synthesis, characterization and applications. Coord Chem Rev 249:1870–1901. https://doi.org/10.1016/j.ccr.2005.01.030
64. Hong X, Tan C, Chen J, Xu Z, Zhang H (2015) Synthesis, properties and applications of one- and two-dimensional gold nanostructures. Nano Res 8:40–55. https://doi.org/10.1007/s12274-014-0636-3
65. Lakowicz JR (2006) Principles of fluorescence spectroscopy, 3rd edn. Springer, Boston, MA. https://doi.org/10.1007/978-0-387-46312-4
66. Dulkeith E, Ringler M, Klar TA, Feldmann J, Javier AM, Parak WJ (2005) Gold nanoparticles quench fluorescence by phase induced radiative rate suppression. Nano Lett 5:585–589. https://doi.org/10.1021/nl0480969
67. Anger P, Bharadwaj P, Novotny L (2006) Enhancement and quenching of single-molecule fluorescence. Phys Rev Lett 96:113002. https://doi.org/10.1103/PhysRevLett.96.113002
68. Sapsford KE, Berti L, Medintz IL (2006) Materials for fluorescence resonance energy transfer analysis: Beyond traditional donor-acceptor combinations. Angew Chemie - Int Ed 45:4562–4589. https://doi.org/10.1002/anie.200503873
69. Ayala-Orozco C, Liu JG, Knight MW, Wang Y, Day JK, Nordlander P, Halas NJ (2014) Fluorescence enhancement of molecules inside a gold nanomatryoshka. Nano Lett 14:2926–2933. https://doi.org/10.1021/nl501027j
70. Baffou G, Quidant R (2013) Thermo-plasmonics: Using metallic nanostructures as nano-sources of heat. Laser Photonics Rev 7:171–187. https://doi.org/10.1002/lpor.201200003
71. Govorov AO, Richardson HH (2007) Generating heat with metal nanoparticles. Nano Today 2:30–38. https://doi.org/10.1016/S1748-0132(07)70017-8
72. Sztandera K, Gorzkiewicz M, Klajnert-Maculewicz B (2019) Gold nanoparticles in cancer treatment. Mol Pharmaceutics 16:1–23. https://doi.org/10.1021/acs.molpharmaceut.8b00810
73. Yavuz MS, Cheng Y, Chen J, Cobley CM, Zhang Q, Rycenga M, Xie J, Kim C, Song KH, Schwartz AG, Wang LV, Xia Y (2009) Gold nanocages covered by smart polymers for controlled release with near-infrared light. Nat Mater 8:935–939. https://doi.org/10.1038/nmat2564
74. Agasti SS, Chompoosor A, You C-C, Ghosh P, Kim CK, Rotello VM (2009) Photoregulated release of caged anticancer drugs from gold nanoparticles. J Am Chem Soc 131:5728–5729. https://doi.org/10.1021/ja900591t
75. Nebu J, Sony G (2018) Understanding plasmonic heat-triggered drug release from gold based nanostructure. J Drug Deliv Sci Technol 46:294–301. https://doi.org/10.1016/j.jddst.2018.05.036
76. Bisker G, Yeheskely-Hayon D, Minai L, Yelin D (2012) Controlled release of Rituximab from gold nanoparticles for phototherapy of malignant cells. J Control Release 162:303–309. https://doi.org/10.1016/j.jconrel.2012.06.030
77. Marangoni VS, Cancino Bernardi J, Reis IB, Fávaro WJ, Zucolotto V (2019) Photothermia and activated drug release of natural cell membrane coated plasmonic gold nanorods and β-Lapachone. ACS Appl Bio Mater 2:728–736. https://doi.org/10.1021/acsabm.8b00603
78. You J, Zhang R, Xiong C, Zhong M, Melancon M, Gupta S, Nick AM, Sood AK, Li C (2012) Effective photothermal chemotherapy using doxorubicin-loaded gold nanospheres that target EphB4 receptors in tumors. Cancer Res 72:4777–4786. https://doi.org/10.1158/0008-5472.CAN-12-1003
79. Nair JB, Joseph MM, Arya JS, Sreedevi P, Sujai PT, Maiti KK (2020) Elucidating a thermoresponsive multimodal photo-chemotherapeutic nanodelivery vehicle to overcome the barriers of doxorubicin therapy. ACS Appl Mater Interfaces 12:43365–43379. https://doi.org/10.1021/acsami.0c08762
80. Liu Q, Zhan C, Kohane DS (2017) Phototriggered drug delivery using inorganic nanomaterials. Bioconjug Chem 28:98–104. https://doi.org/10.1021/acs.bioconjchem.6b00448
81. Jaque D, Martínez Maestro L, del Rosal B, Haro-Gonzalez P, Benayas A, Plaza JL, Martín Rodríguez E, J. García Solé J, (2014) Nanoparticles for photothermal therapies. Nanoscale 6:9494–9530. https://doi.org/10.1039/c4nr00708e
82. Wei W, Zhang X, Zhang S, Wei G, Su Z (2019) Biomedical and bioactive engineered nanomaterials for targeted tumor

photothermal therapy: A review. Mater Sci Eng C 104:109891. https://doi.org/10.1016/j.msec.2019.109891
83. Hu Q, Huang Z, Duan Y, Fu Z, Liu B (2020) Reprogramming tumor microenvironment with photothermal therapy. Bioconjug Chem 31:1268–1278. https://doi.org/10.1021/acs.bioconjchem.0c00135
84. Huang X, Jain PK, El-Sayed IH, El-Sayed MA (2008) Plasmonic photothermal therapy (PPTT) using gold nanoparticles. Lasers Med Sci 23:217–228. https://doi.org/10.1007/s10103-007-0470-x
85. Ayala-Orozco C, Urban C, Knight MW, Urban AS, Neumann O, Bishnoi SW, Mukherjee S, Goodman AM, Charron H, Mitchell T, Shea M, Roy R, Nanda S, Schiff R, Halas NJ, Joshi A (2014) Au nanomatryoshkas as efficient near-infrared photothermal transducers for cancer treatment: Benchmarking against nanoshells. ACS Nano 8:6372–6381. https://doi.org/10.1021/nn501871d
86. Rastinehad AR, Anastos H, Wajswol E, Winoker JS, Sfakianos JP, Doppalapudi SK, Carrick MR, Knauer CJ, Taouli B, Lewis SC, Tewari AK, Schwartz JA, Canfield SE, George AK, West JL, Halas NJ (2019) Gold nanoshell-localized photothermal ablation of prostate tumors in a clinical pilot device study. Proc Natl Acad Sci U S A 116:18590–18596. https://doi.org/10.1073/pnas.1906929116
87. Cherukuri P, Glazer ES, Curley SA (2010) Targeted hyperthermia using metal nanoparticles. Adv Drug Deliv Rev 62:339–345. https://doi.org/10.1016/j.addr.2009.11.006
88. Song C, Li F, Guo X, Chen W, Dong C, Zhang J, Zhang J, Wang L (2019) Gold nanostars for cancer cell-targeted SERS-imaging and NIR light-triggered plasmonic photothermal therapy (PPTT) in the first and second biological windows. J Mater Chem B 7:2001–2008. https://doi.org/10.1039/c9tb00061e
89. Il Choi W, Kim J-Y, Kang C, Byeon CC, Kim YH, Tae G (2011) Tumor regression in vivo by photothermal therapy based on gold-nanorod-loaded, functional nanocarriers. ACS Nano 5:1995–2003. https://doi.org/10.1021/nn103047r
90. Jain PK, ElSayed IH, El-Sayed MA (2007) Au nanoparticles target cancer. Nano Today 2:18–29. https://doi.org/10.1016/S1748-0132(07)70016-6
91. Tabish TA, Dey P, Mosca S, Salimi M, Palombo F, Matousek P, Stone N (2020) Smart gold nanostructures for light mediated cancer theranostics: Combining optical diagnostics with photothermal therapy. Adv Sci 7:1903441. https://doi.org/10.1002/advs.201903441
92. Her S, Jaffray DA, Allen C (2017) Gold nanoparticles for applications in cancer radiotherapy: Mechanisms and recent advancements. Adv Drug Deliv Rev 109:84–101. https://doi.org/10.1016/j.addr.2015.12.012
93. Mantri Y, Jokerst JV (2020) Engineering plasmonic nanoparticles for enhanced photoacoustic imaging. ACS Nano 14:9408–9422. https://doi.org/10.1021/acsnano.0c05215
94. Li W, Chen X (2015) Gold nanoparticles for photoacoustic imaging. Nanomedicine 10:299–320. https://doi.org/10.2217/nnm.14.169
95. Mieszawska AJ, Mulder WJM, Fayad ZA, Cormode DP (2013) Multifunctional gold nanoparticles for diagnosis and therapy of disease. Mol Pharmaceutics 10:831–847. https://doi.org/10.1021/mp3005885
96. Quintana C, Cifuentes MP, Humphrey MG (2020) Transition metal complex/gold nanoparticle hybrid materials. Chem Soc Rev 49:2316–2341. https://doi.org/10.1039/c9cs00651f
97. Glomm WR, Moses SJ, Brennaman MK, Papanikolas JM, Franzen S (2005) Detection of adsorption of Ru(II) and Os(II) polypyridyl complexes on gold and silver nanoparticles by single-photon counting emission measurements. J Phys Chem B 109:804–810. https://doi.org/10.1021/jp049184k
98. Pramod P, Sudeep PK, Thomas KG, Kamat PV (2006) Photochemistry of ruthenium trisbipyridine functionalized on gold nanoparticles. J Phys Chem B 110:20737–20741. https://doi.org/10.1021/jp064878
99. Huang T, Murray RW (2002) Quenching of $[Ru(bpy)_3]^{2+}$ fluorescence by binding to Au nanoparticles. Langmuir 18:7077–7081. https://doi.org/10.1021/la025948g
100. Leung FC-M, Tam AY-Y, Au VK-M, Li M-J, Yam VW-W (2014) Förster resonance energy transfer studies of luminescent gold nanoparticles functionalized with ruthenium(II) and rhenium(I) complexes: Modulation via esterase hydrolysis. ACS Appl Mater Interfaces 6:6644–6653. https://doi.org/10.1021/am500350c
101. Miomandre F, Stancheva S, Audibert J-F, Brosseau A, Pansu RB, Lepeltier M, Mayer CR (2013) Gold and silver nanoparticles functionalized by luminescent iridium complexes: Synthesis and photophysical and electrofluorochromic properties. J Phys Chem C 117:12806–12814. https://doi.org/10.1021/jp312625x
102. Osborne SAM, Pikramenou Z (2015) Highly luminescent gold nanoparticles: Effect of ruthenium distance for nanoprobes with enhanced lifetimes. Faraday Discuss 185:219–231. https://doi.org/10.1039/c5fd00108k
103. King SM, Claire S, Teixeira RI, Dosumu AN, Carrod AJ, Dehghani H, Hannon MJ, Ward AD, Bicknell R, Botchway SW, Hodges NJ, Pikramenou Z (2018) Iridium nanoparticles for multichannel luminescence lifetime imaging, mapping localization in live cancer cells. J Am Chem Soc 140:10242–10249. https://doi.org/10.1021/jacs.8b05105
104. Rogers NJ, Claire S, Harris RM, Farabi S, Zikeli G, Styles IB, Hodges NJ, Pikramenou Z (2014) High coating of Ru(II) complexes on gold nanoparticles for single particle luminescence imaging in cells. Chem Commun 50:617–619. https://doi.org/10.1039/c3cc47606e
105. Yu Y, Wu Y, Liu J, Liu Y, Wu D (2017) Highly efficient dual-modal phosphorescence/computed tomography bioprobes based on an iridium complex and AuNP polyiohexol composite nanoparticles. Nanoscale 9:9447–9456. https://doi.org/10.1039/c7nr03185h
106. Ricciardi L, Martini M, Tillement O, Sancey L, Perriat P, Ghedini M, Szerb EI, Yadav YJ, La Deda M (2014) Multifunctional material based on ionic transition metal complexes and gold-silica nanoparticles: Synthesis and photophysical characterization for application in imaging and therapy. J Photochem Photobiol B Biol 140:396–404. https://doi.org/10.1016/j.jphotobiol.2014.09.005
107. Zhang P, Wang J, Huang H, Yu B, Qiu K, Huang J, Wang S, Jiang L, Gasser G, Ji L, Chao H (2015) Unexpected high photothermal conversion efficiency of gold nanospheres upon grafting with two-photon luminescent ruthenium(II) complexes: A way towards cancer therapy? Biomaterials 63:102–114. https://doi.org/10.1016/j.biomaterials.2015.06.012
108. Zhang P, Wang J, Huang H, Qiu K, Huang J, Ji L, Chao H (2017) Enhancing the photothermal stability and photothermal efficacy of AuNRs and AuNTs by grafting with Ru(II) complexes. J Mater Chem B 5:671–678. https://doi.org/10.1039/c6tb01991a
109. Ricciardi L, Sancey L, Palermo G, Termine R, De Luca A, Szerb EI, Aiello I, Ghedini M, Strangi G, La Deda M (2017) Plasmon-mediated cancer phototherapy: The combined effect of thermal and photodynamic processes. Nanoscale 9:19279–19289. https://doi.org/10.1039/c7nr05522f
110. Xiong C, Lu W, Zhou M, Wen X, Li C (2018) Cisplatin-loaded hollow gold nanoparticles for laser-triggered release. Cancer Nanotechnol 9:6. https://doi.org/10.1186/s12645-018-0041-9
111. Guan Y-H, Tian M, Liu X-Y, Wang Y-N (2019) Preparation of novel cisplatin-conjugated hollow gold nanospheres for targeting cervical cancer. J Cell Physiol 234:16475–16484. https://doi.org/10.1002/jcp.28316

112. Feng B, Xu Z, Zhou F, Yu H, Sun Q, Wang D, Tang Z, Yu H, Yin Q, Zhang Z, Li Y (2015) Near infrared light-actuated gold nanorods with cisplatin-polypeptide wrapping for targeted therapy of triple negative breast cancer. Nanoscale 7:14854–14864. https://doi.org/10.1039/c5nr03693c
113. Gao J, Wang F, Wang S, Liu L, Liu K, Ye Y, Wang Z, Wang H, Chen B, Jiang J, Ou J, van Hest JCM, Peng F, Tu Y (2020) Hyperthermia-triggered on-demand biomimetic nanocarriers for synergetic photothermal and chemotherapy. Adv Sci 7:1903642. https://doi.org/10.1002/advs.201903642
114. Shanmugam V, Chien Y-H, Cheng Y-S, Liu T-Y, Huang C-C, Su C-H, Chen Y-S, Kumar U, Hsu H-F, Yeh C-S (2014) Oligonucleotides-assembled au nanorod-assisted cancer photothermal ablation and combination chemotherapy with targeted dual-drug delivery of doxorubicin and cisplatin prodrug. ACS Appl Mater Interfaces 6:4382–4393. https://doi.org/10.1021/am5000905
115. Shi S, Chen X, Wei J, Huang Y, Weng J, Zheng N (2016) Platinum(IV) prodrug conjugated Pd@Au nanoplates for chemotherapy and photothermal therapy. Nanoscale 8:5706–5713. https://doi.org/10.1039/c5nr09120a
116. Zhang Y, Liu Z, Thackray BD, Bao Z, Yin X, Shi F, Wu J, Ye J, Di W (2018) Intraoperative Raman-guided chemo-photothermal synergistic therapy of advanced disseminated ovarian cancers. Small 14:1801022. https://doi.org/10.1002/smll.201801022
117. Zhang L, Su H, Cai J, Cheng D, Ma Y, Zhang J, Zhou C, Liu S, Shi H, Zhang Y, Zhang C (2016) A multifunctional platform for tumor angiogenesis-targeted chemo-thermal therapy using polydopamine-coated gold nanorods. ACS Nano 10:10404–10417. https://doi.org/10.1021/acsnano.6b06267
118. Yu S, Huang G, Yuan R, Chen T (2020) A uPAR targeted nanoplatform with an NIR laser-responsive drug release property for trimodal imaging and synergistic photothermal-chemotherapy of triple-negative breast cancer. Biomater Sci 8:720–738. https://doi.org/10.1039/c9bm01495k
119. Luo G-F, Chen W-H, Lei Q, Qiu W-X, Liu Y-X, Cheng Y-J, Zhang X-Z (2016) A triple-collaborative strategy for high-performance tumor therapy by multifunctional mesoporous silica-coated gold nanorods. Adv Funct Mater 26:4339–4350. https://doi.org/10.1002/adfm.201505175
120. Mirrahimi M, Beik J, Mirrahimi M, Alamzadeh Z, Teymouri S, Mahabadi VP, Eslahi N, Ebrahimi Tazehmahalleh F, Ghaznavi H, Shakeri-Zadeh A, Moustakis C (2020) Triple combination of heat, drug and radiation using alginate hydrogel co-loaded with gold nanoparticles and cisplatin for locally synergistic cancer therapy. Int J Biol Macromol 158:617–626. https://doi.org/10.1016/j.ijbiomac.2020.04.272
121. Elmes RBP, Orange KN, Cloonan SM, Williams DC, Gunnlaugsson T (2011) Luminescent ruthenium(II) polypyridyl functionalized gold nanoparticles; Their DNA binding abilities and application as cellular imaging agents. J Am Chem Soc 133:15862–15865. https://doi.org/10.1021/ja2061159
122. Graf N, Bielenberg DR, Kolishetti N, Muus C, Banyard J, Farokhzad OC, Lippard SJ (2012) $\alpha_v\beta_3$ integrin-targeted PLGA-PEG nanoparticles for enhanced anti-tumor efficacy of a Pt(IV) prodrug. ACS Nano 6:4530–4539. https://doi.org/10.1021/nn301148e
123. Xiao H, Qi R, Liu S, Hu X, Duan T, Zheng Y, Huang Y, Jing X (2011) Biodegradable polymer-cisplatin(IV) conjugate as a pro-drug of cisplatin(II). Biomaterials 32:7732–7739. https://doi.org/10.1016/j.biomaterials.2011.06.072